

Visualizing Conformations in Molecular Dynamics

Christoph Best*, Hans-Christian Hege

March 1999

Abstract

The Monte Carlo simulation of the dynamics of complex molecules produces trajectories with a large number of different configurations to sample configuration space. It is expected that these configurations can be classified into a small number of conformations representing essential changes in the shape of the molecule. We present a method to visualize these conformations by point sets in the plane based on a geometrical distance measure between individual configurations. It turns out that different conformations appear as well-separated point sets. The method is further improved by performing a cluster analysis of the data set. The point-cluster representation is used to control a three-dimensional molecule viewer application to show individual configurations and conformational changes. The extraction of essential coordinates and visualization of molecular shape is discussed.

I Introduction

Molecular dynamics simulations on large computers have become one of the mainstays for investigating the functions of biomolecules. Using statistical algorithms, they create a large number of snapshots of the molecule that approximate the expected distribution of molecular shapes in actual molecular processes. By looking for typical shapes (conformations) and transition paths in this large data set, biochemists can learn about the molecular bases of biochemical processes. Such understanding is important in particular in designing more efficient medical drugs.

Identifying typical shapes in such a large data set is itself a difficult task [1]. In most simulation, one focuses on a few characteristic numbers, like the angles or distances between specific atoms in the molecule, and monitors the change of these quantities in the simulation. This approach requires some advance knowledge about which parts of the molecule are important to the dynamics, and makes it also difficult to perform the analysis automatically.

To use all the information computed in a molecular dynamics simulation, one must leave the analysis step again to a computer. We present here two procedures

* current address: John von Neumann Institute for Computing, 54245 Jülich, Germany.

E-Mail: *c.best@computer.org*

Keywords: Molecular Dynamics, Conformations, Visualization, Cluster Analysis.

MSC: 62-07, 92E10, 92C40 PACS: 07.05.Rm, 87.15.He

to aid in this task: a projection method to visualize the molecular configurations of a trajectory as a point set in the plane, and a cluster analysis to identify clusters of similar configurations in the trajectory. These methods can be applied automatically to any molecular dynamics trajectory and result in a tentative identification of conformations in the trajectory.

II Procedure

II.1 Configurations and feature vectors

The output of a molecular dynamics simulation is a trajectory, i.e. sequence of configurations that depicts the evolution of the molecule in time. If the molecule consists of n atoms, the configuration x is described by n 3-dimensional vectors $\mathbf{x}_i \in \mathbf{R}^3$ that specify the cartesian position of each atom in 3-dimensional space. Other information, in particular which atoms are connected by chemical bonds, is a property of the molecule and usually does not change during the simulation.

To classify the configurations, we must quantify how much their geometries differ. We thus assign to each configuration a feature vector that describes the geometry of the configuration in such a way that similar configurations have similar feature vectors. However, the set of $3n$ numbers that make up the cartesian positions of the atoms is unsuited as identical geometries can appear with different rotations and translations. While the translational freedom can easily be fixed by requiring that the center of mass coincides with the origin of the coordinate frame, the rotational degree of freedom is extremely difficult to eliminate. Fixing the axis of inertia can lead to sudden artificial rotations when the axes become degenerate, while fixing certain atoms to the coordinate axes always introduces a undesirable bias.

A feature vector that is invariant under translations and rotations and does not introduce any bias can be chosen by considering the set of intramolecular distances [2]

$$\{d_{ij}(x) = |\mathbf{x}_i - \mathbf{x}_j|, \quad i, j \in 1, \dots, n\} \quad . \quad (1)$$

The price to pay is that instead of $3n$ elements, this vector has now $n(n-1)/2$, but geometrically identical configurations have identical feature vectors, and the cartesian distance in $n(n-1)/2$ -dimensional space is a natural measure of conformational distance:

$$d(x, y) = \sqrt{\frac{1}{n(n-1)/2} \sum_{i>j} (d_{ij}(x) - d_{ij}(y))^2} \quad . \quad (2)$$

Another frequent way to choose a feature vector is to use the dihedral angles between certain atoms as basic degrees of freedom. This is a natural choice as dihedral angles are the main degrees of motion in the simulations (atomic distances and bond angles are usually much more rigid). However, the potential energy that determines the dynamics of the molecule depends on the spatial distance of the atoms, and the

relation between dihedral angles and spatial distances is involved at best. We prefer here to put all information as unbiased as possible to the algorithm and depend on it to extract the relevant degrees of freedom.

The feature vector (1) is vast compared to the number of degrees of freedom (in our example molecule, it has 2415 elements as compared to $70 \times 3 - 6 = 204$ degrees of freedom). Some of its elements will show little or no fluctuation (e.g. the ones associated to the lengths of chemical bonds), others will fluctuate thermally, and still others will assume different values in different fluctuations and thus exhibit a double-peaked distribution. To reduce the thermal noise, we analyze the elements of the feature vector statistically and select those whose distribution has the largest width. As thermal fluctuations are smaller than the conformational changes, this also selects the distances most affected by conformational changes. A similar procedure has been used by [3] to identify essential degrees of freedom in cartesian coordinate space.

II.2 Low-dimensional approximations

The feature vector space is by far too large to be visualized directly. To capture the major properties of the point set that represents a trajectory in this space, we seek to visualize it in a plane, i.e. to assign each configuration a point in the two-dimensional plane such that the geometrical similarity between configurations is reproduced as faithfully as possible. After having chosen a distance measure (2) on the trajectory, this reduces to the general problem of visualizing an arbitrary distance matrix D_{ij} between a set of N configurations, where i and j now number configurations.

One choice is to require that the mean quadratic deviation of the conformational distance from the distance in the plane, given by

$$D^2 = \sum_{i>j} (|\mathbf{x}_i - \mathbf{x}_j| - D_{ij}) \quad (3)$$

is minimized by the choice of the points \mathbf{x}_i , i.e. that the derivative of the quantity with respect to the position of the k -th point

$$\frac{\partial D^2}{\partial \mathbf{x}_k} = \sum_i \frac{\mathbf{x}_k - \mathbf{x}_i}{|\mathbf{x}_k - \mathbf{x}_i|} (|\mathbf{x}_k - \mathbf{x}_i| - d_{ik}) = 0 \quad (4)$$

vanishes. This equation can be pictured physically by a set of springs that connect the points and whose natural length is given by the desired distance between the points.

We solve the minimum problem of (3) numerically by the conjugate-gradient method. Though there is no guarantee that the minimum found by this method is the global one, the minimization takes place in a $2N$ -dimensional space where it is improbable that a false minimum is stable in all directions. An example of this is the situation where we have a solution of Eq. (4) in $D - 1$ dimensions and then extend the solution space to D dimensions by setting $x_{i,D} = 0$ for all i , which still satisfies Eq. (4). However, this minimum (in $D - 1$ dimensions) now turns out to be a saddle point in D

dimensions, where the second derivative of D^2 is

$$\frac{\partial D^2}{\partial x_{k,D} \partial x_{l,D}} = \begin{cases} \frac{d_{kl} - |\mathbf{x}_k - \mathbf{x}_l|}{|\mathbf{x}_k - \mathbf{x}_l|} & \text{if } k \neq l \\ -\sum_{i \neq k} \frac{d_{ki} - |\mathbf{x}_k - \mathbf{x}_i|}{|\mathbf{x}_k - \mathbf{x}_i|} & \end{cases} \quad (5)$$

In a true minimum, this quantity is positive, thus requiring that

$$d_{kl} \geq |\mathbf{x}_k - \mathbf{x}_l| \quad \text{for all } k, l \quad (6)$$

but also

$$\sum_{i \neq k} \frac{d_{ki} - |\mathbf{x}_k - \mathbf{x}_i|}{|\mathbf{x}_k - \mathbf{x}_i|} \leq 0 \quad \text{for all } k \quad (7)$$

This will happen only if the first inequality is an equality, i.e. if the solution is complete.

Another widely used low-dimensional approximation is based on the singular-value decomposition (SVD) of the feature matrix [4]. Let a_{ij} be the feature matrix of $i = 1, \dots, n$ objects with $j = 1, \dots, m$ features each. (In our example, n is the number of configurations while m is the number of intramolecular distances.) The singular-value decomposition expresses this matrix as a series

$$a_{ij} = \sum_k \lambda_k u_i^{(k)} v_j^{(k)} \quad (8)$$

where $\mathbf{u}^{(k)}$ and $\mathbf{v}^{(k)}$ are n - and m -dimensional, resp., orthonormalized basis vectors, and λ_k gives the weight of k -th term. The number of terms in the series is the rank of the matrix, it is at most the lower of n and m .

The relation between singular-value decomposition and point sets in low-dimensional space can be seen by calculating the distance between feature vectors in terms of the SVD:

$$\begin{aligned} D_{ij} &= \sum_k (a_{ik} - a_{jk})^2 \\ &= \sum_k \left(\sum_l \lambda_l (u_i^{(l)} - u_j^{(l)}) v_k^{(l)} \right)^2 \\ &= \sum_k \lambda_k^2 (u_i^{(k)} - u_j^{(k)})^2 \end{aligned} \quad (9)$$

when orthonormality of $v^{(k)}$ is taken into account. Thus the vectors

$$\{\lambda_k u_i^{(k)} : k = 1, \dots, m\} \quad (10)$$

can be interpreted as specifying the cartesian positions in m -dimensional space of the i -th data point. When we chose λ_k in decreasing order, truncating the series after singular-value decomposition after l terms will lead position vectors in l -dimensional space that are best approximations in a linear sense.

The major difference between the two approaches is that the SVD performs the approximation in a linear manner: When the dimension of the approximation space is

decreased from D to $D - 1$, the new approximation is simply obtained by orthogonally projecting out the last coordinate. In contrast, in the approximation obtained from minimizing (3), the nonlinearity introduced by the square root redistributes some of the “lost” distance in the remaining dimensions.

II.3 Cluster analysis

Cluster analysis [5, 6] is a statistical method to partition the point set into disjoint subsets with the property that the points in a subset are in some sense closer to each other than to the remaining points. There are several different ways to make this statement mathematically precise. We choose the notion of minimum residual similarity between clusters which leads to a natural formulation of the problem in terms of eigensystem analysis and to a heuristic algorithm for its solution. This spectral method goes back to works by Donath and Hoffmann [7, 8] on graph partitioning in computer logic and Fiedler [9, 10] on acyclic graphs and was later picked up by Hendrickson [16]. Other cluster analysis methods based on neural networks or fuzzy clustering have also been applied to molecular dynamics simulations [11, 12].

Amadei *et.al.* [3] went further by introducing the concept of essential dynamics in which the coordinate space of the molecule is split into a small essential subspace and a larger non-essential subspace. They assumed a linear factorization of the coordinate space and identified essential coordinates by large second moments of their distribution, assuming that these distributions are mainly non-Gaussian double-peaked shapes.

To be as flexible as possible, we assume that a similarity measure

$$0 \leq a_{ij} \leq 1, \quad 1 \leq i \leq n \quad (11)$$

is given between the n data points, where $a_{ij} = 0$ indicates complete dissimilarity and $a_{ij} = 1$ complete identity of configurations i and j . The residual similarity of a cluster $C \subset \{1, \dots, n\}$ characterizes how similar elements of the cluster are to elements outside the cluster

$$R(C) = \sum_{i \in C, j \notin C} A_{ij} \quad (12)$$

We wish to partition the data set into two subsets such that this quantity is minimized. Let a_i the characteristic vector of this partition, with value $a_i = 1$ indicating that $i \in C$, and otherwise $a_i = -1$. Then the residual similarity can be rewritten

$$\begin{aligned} R(C) &= \frac{1}{4} \sum_{ij} (a_i - a_j)^2 A_{ij} \\ &= \frac{1}{2} \sum_{ij} a_i \left(\sum_k A_{ik} \delta_{ij} - A_{ij} \right) a_j \\ &= (a, Ma) \end{aligned} \quad (13)$$

with the Laplacian matrix

$$M_{ij} = \begin{cases} -A_{ij} & \text{if } i \neq j \\ \sum_k A_{ik} & \text{if } i = j \end{cases} \quad (14)$$

To find the minimum of the expectation value (a, Ma) over the vectors that have element ± 1 only, is a hard combinatorial problem. However, if we relax the problem and allow real values for the a_i with the constraint $|a_i| = 1$, the problem is exactly the problem of finding the second-lowest eigenvector of the matrix M (the lowest eigenvector corresponds to the solution $a_i \equiv 1$ that does not lead to a proper partition). Since eigenvectors are orthogonal, the second-lowest eigenvector satisfies

$$\sum_i a_i^2 = 1 \quad \text{and} \quad \sum_i a_i = 0 \quad (15)$$

and thus guarantees that it will contain both positive and negative eigenvalues. In graph theory, this eigenvector is called the characteristic valuation of a graph.

Low-lying eigenvectors of a matrix can be found using iterative methods even for moderately large matrices. There is, however, no safe way to recover the solution of the combinatorial problem, where a is restricted to values of ± 1 from it, but it can be argued that for most matrices the eigenvector will constitute a good approximation to the combinatorial problem. We thus map the continuous value a_i to discrete value \tilde{a}_i using a threshold l :

$$\tilde{a}_i = \begin{cases} -1 & \text{if } a_i \leq l \\ +1 & \text{if } a_i > l \end{cases} \quad (16)$$

The threshold can now be determined by minimizing the residual similarity over all possible thresholds. In this way, the minimization problem is reduced from $n!$ to just n options, and the characteristic valuation serves as a heuristic to determine the options that are taken into consideration.

The measure of residual similarity favors in general splitting off a single point from the data set since (13) contains in this case only $n - 1$ terms, as compared to $n^2/4$ when splitting symmetrically. This automatically introduces a quality control in the splits, as central splits occur only when the cluster separation is rather favorable, but might also hinder the analysis of noisy data. However, the special form (13) was only chosen to turn the problem into an eigenvalue problem. As the whole procedure is heuristic in nature, we may well decide to use a different similarity measure when determining the splitting threshold, e.g. a measure that includes a combinatorial factor

$$R(C) = \frac{1}{|C|(n - |C|)} \left| \sum_{i \in C, j \notin C} A_{ij} \right| \quad (17)$$

Which measure is correct depends mainly on the application. The original measure is stricter in what it returns as a cluster, while the latter measure favors balanced splittings. In some problems, like partitioning matrices for processing in a parallel computer, one may even demand that each split is symmetrical.

Another approach taken frequently in cluster analysis is to use the singular-value decomposition [13]. If we go back to the feature matrix A_{ij} and its singular value decomposition (8), it turns out that the vectors $u^{(l)}$ correspond to minima of the expectation value with respect to the feature matrix squared, i.e.

$$\sum_k \left(\sum_i u_i A_{ik} \right)^2 = \sum_{ij} u_i (A_i \cdot A_j) u_j \quad (18)$$

where we introduced the row vectors A_i of the matrix A_{ik} , i.e. the feature vector of data point i . Thus in this approach the role of the similarity matrix is taken over by the scalar-product matrix of the feature vectors. The major differences are

1. The scalar products are not less than or equal to one, but this could easily be fixed by globally rescaling the scalar-product matrix, which does not change the vectors $u^{(l)}$.
2. The scalar products can be negative. The notion of a scalar-product is not of similarity and dissimilarity but rather the trichotomy of similar, orthogonal, and antagonistic.

Thus, singular-value decomposition seems suitable for feature vectors that characterize orthogonal qualities. However, this is not the case in our feature vectors, so we chose a similarity measure based upon distance.

After partitioning the data set into two subsets, we proceed to apply the algorithm again to these subsets. In this way, one obtains a splitting tree that terminates only when the subset size is smaller than three. For many applications, such a tree is already quite useful as it orders the data points in such a way to similar data points are usually close to each other.

To identify clusters in the splitting tree, we found that the average width of the cluster relative to that of its parent cluster gives the best indication. To calculate the average width of a cluster we use the Euclidean distance in the high-dimensional space and average over all distinct pairs of points in a cluster. This quantity relative to that of the parent cluster basically indicates how much the closer the points are on average in the subcluster than in the original cluster and thus how much the split improves the cluster criterion. Consider e.g. the situation where there are three clusters. The first split will result in one correctly identified cluster and a second pseudo-cluster that encompasses the other two, but the relative width of the true cluster will be much smaller than that of the pseudo-cluster. Only after the next split it will be revealed that the latter consists of two clusters. Typical values for this quantity are between 0.5 and 0.8.

III Results

We apply our methods to a molecular dynamics simulation of the molecule *adenylyl(3'-5')cytidylyl(3'-5')cytidin* in vacuum [14]. This is a very simple tri-ribonucleotide, consisting of three residues and 70 (effective) atoms. The simulation was performed using the GROMOS96 [15] extended atom force field. For the analysis, we chose a subset of 1000 configurations equidistantly from the trajectory.

Fig. 1 shows the two-dimensional map of the trajectory found by minimizing (3). The points are connected by a line in the same sequence as they are generated in the Monte Carlo simulation. This information does not enter in determining the locations

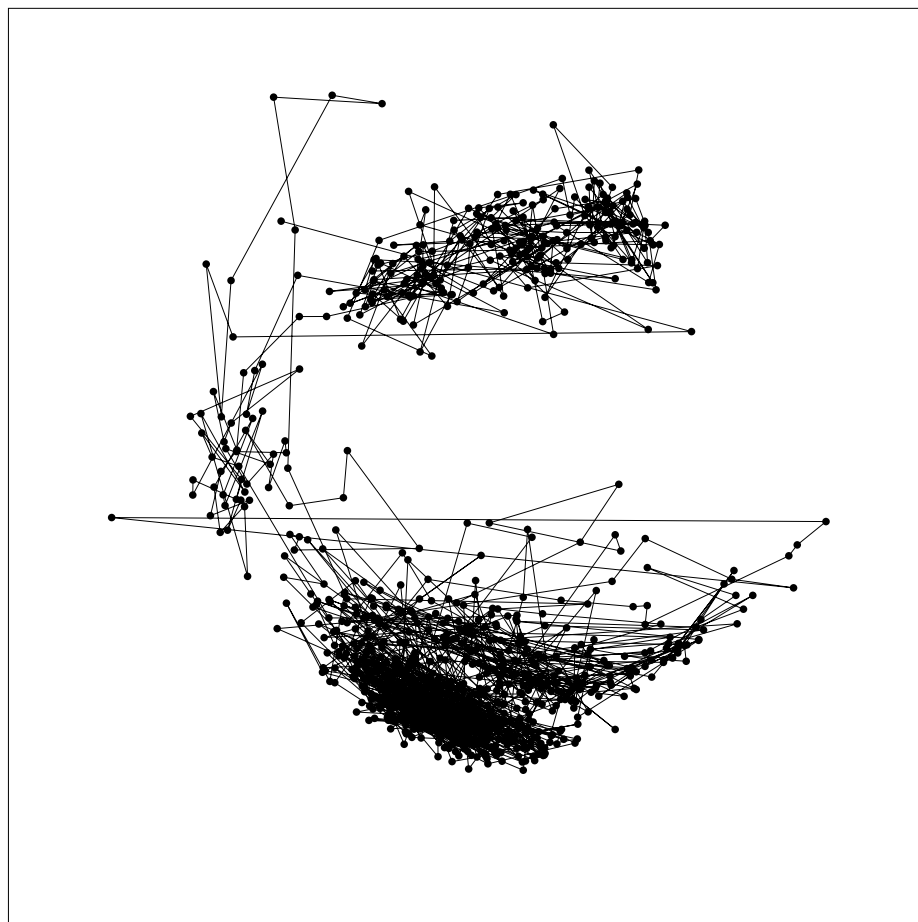


Figure 1: Two-dimensional map of 1000 configurations chosen from a molecular dynamics trajectory

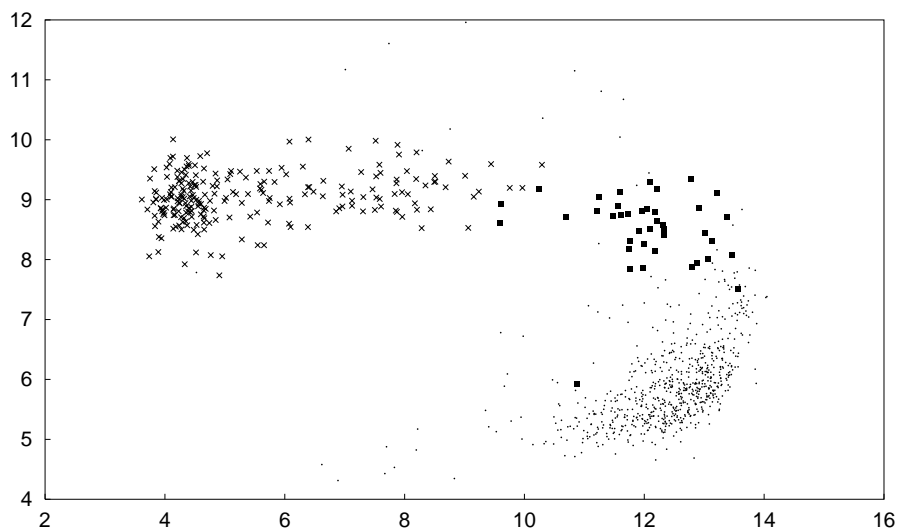


Figure 2: Map of the trajectory in the plane spanned by two typical distances in the molecule

of the points in the plane, so the fact that the line segments are rather short indicates that point adjacent in the trajectory are mapped to nearby points in the plane and thus are recognized as geometrically similar by the algorithm. The one pair of lines that crosses nearly the whole plane horizontally is actually made up of the first three data points and therefore a transient effect before the molecule became equilibrated.

We immediately notice that there are at least three clearly different groups of points which constitute conformations in a geometrical sense, i.e. subsets of the trajectory with similar geometrical properties. That they are also dynamical conformations can be seen from the fact that the connecting line of the points only very rarely crosses from one point group into the next. This again confirms that the two-dimensional layout in the plane chosen by the algorithm represents correctly the dynamics of the system.

The representation of Fig. 1 can be compared to a representation where the dimensionality of the system is reduced by chemical understanding. As the system consists of three residues, most of the conformational dynamics can be assumed to be in the geometrical layout of the residues. This can be described by only three numbers, and we chose two of them to create the two-dimensional representation shown in Fig. 2. This picture is similar to Fig. 1 in that there appear approximately three distinct point groups, and it can be verified that they correspond to the point groups from Fig. 1. However, the separation of the point groups is less clear than in Fig. 1. This indicates that the conformational dynamics is not simply the motion of the *centers* of the residues, but there are also smaller rearrangements in the residues themselves that are correlated to the large-scale motions. By considering an unbiased measure for geometrical similarity, all those little rearrangements enter and reinforce the distance between conformations in the plane.

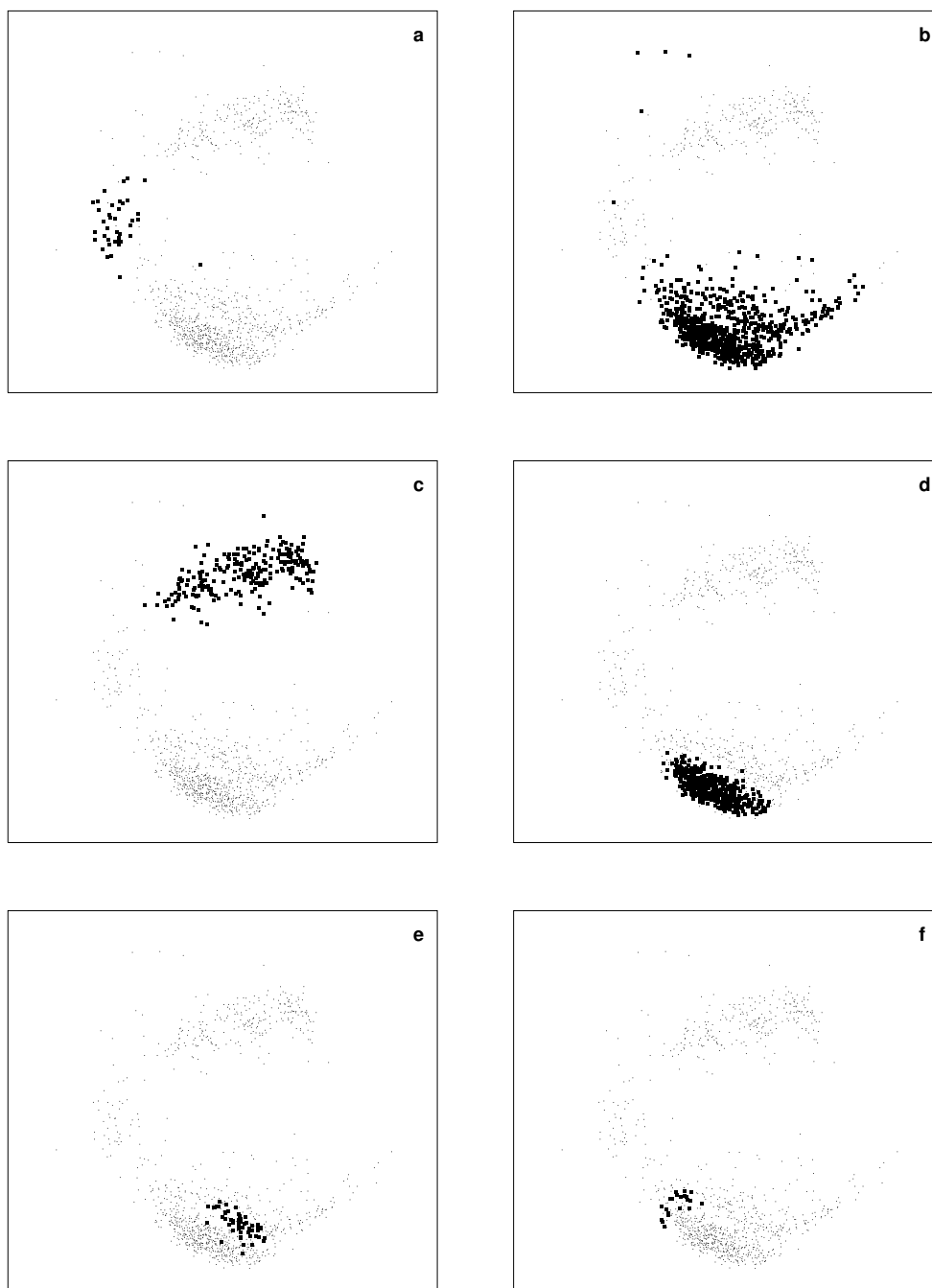


Figure 3: Different clusters identified in the trajectory by the clustering algorithm. Figures a, b, and c show the decomposition of the trajectory into three conformational clusters , while d, e, and f show the substructure of one such cluster.

III.1 Cluster analysis

Applying the cluster algorithm to the similarity matrix of the trajectory, the first few splits remove 22 isolated points before the small cluster shown in Fig. 3a with 40 points and a relative width of 0.46 (both compared to its immediate predecessor and to the initial point set) shows up. The remaining points are split some steps further into a cluster with 698 points shown in Fig. 3b and another cluster with 230 points shown in Fig. 3c with relative widths of about 0.53. After some more steps, the larger subcluster is broken into three subclusters with 388, 52, and 21 points, resp., and relative widths of 0.91, 0.73, and 0.61, resp., as shown in Fig. 3d, e, and f. Similarly, the smaller subcluster also separates into three weak subclusters.

The splitting line of the large cluster at the bottom is also visible in Fig. 1. Such a pattern usually indicates that beside a large conformational change that induces the three clearly visible clusters, where the middle cluster is clearly a transitional state, there is another smaller conformational change, possibly in one of the glucose rings, independent of the larger one. As it only affects a small part of the molecule, the conformational distance is smaller and is then imprinted like a fine structure on the clusters. That such changes are visible in the plot is an advantage from considering all atom coordinates without bias.

IV Conclusions and Outlook

We have demonstrated a method for projecting a molecular dynamics trajectory onto a plane to capture the conformational structure of the trajectory. Conformations can in this way be easily identified by visual inspection. Cluster analysis on the full conformational distance matrix also revealed these clusters, but also allowed to discern fine structure inside the clusters caused by smaller conformational changes.

To simplify the analysis of a trajectory, we have created a Java application that reads the output files of the combined plane mapping/cluster analysis program and displays the two-dimensional map. This program interacts directly with an Open Inventor molecular visualization application by means of a Unix pipe. Whenever the user selects a point in the plane, the corresponding configuration is shown in the visualization program. The user can also choose to display identified clusters using different colors in the map.

Identifying which parts of the molecule are responsible for different conformations is a much more difficult problem. We use a visualization application that allows the user to form groups of atoms that are visualized by ellipsoids. In this way, a molecule can be easily reduced to its functional groups where it is much easier to spot conformational changes. However, small conformational changes as those that show up as a fine structure on the plane map are easily lost in this representation.

As a first attempt at aiding the eye in discovering unusual motions of the molecule, we implemented a simple OpenGL effect in the visualization application that allows to

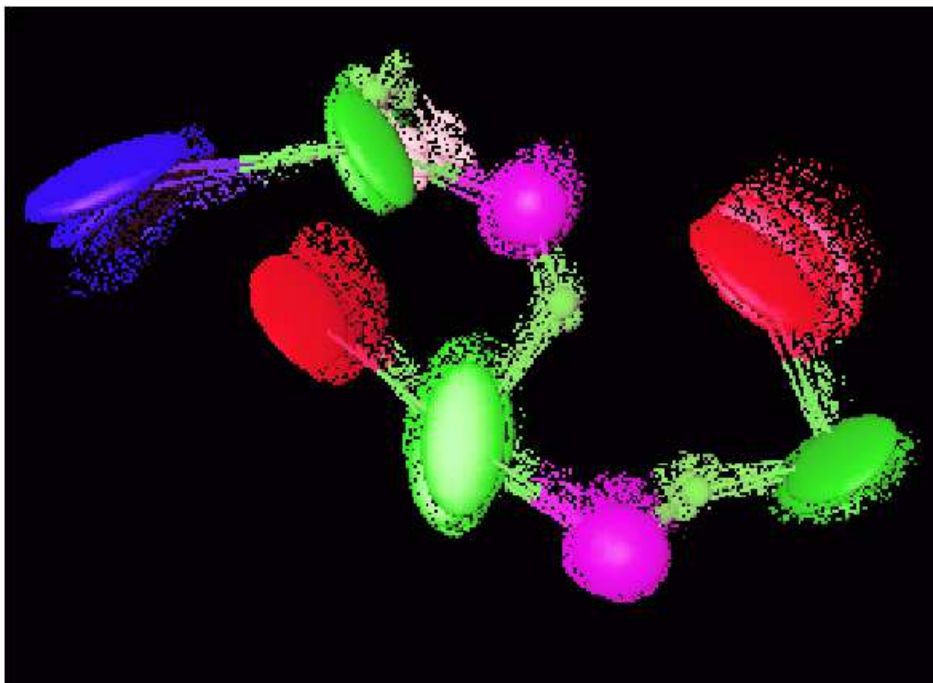


Figure 4: Representation of the collective motion by an OpenGL fading effect

blend several frames of an animation in the hope that large changes stand out more clearly in this representation. Fig. 4 shows one such picture. Certainly more research can be expended on how to identify and visualize the essential degrees of freedoms.

The concept of essential molecular dynamics has been introduced to reduce the number of degrees of freedom in the simulation. Both the plane map and the cluster analysis can be used to inflict new coordinates upon the system. For the point map, these are simply the x and y positions of the configuration in the plane. Once a certain point map has been established, new configurations can be fitted into the plane by minimizing the residual distance while keeping all other points fixed. Similarly, the cluster analysis assigns to each configuration a position in the tree that can be seen as a (discrete) essential coordinate. How such essential coordinates can be reintroduced into the dynamics of the system is still an open question.

References

- [1] W. Huisinga, C. Best, R. Roitzsch, C. Schütte, F. Cordes, *From Simulation Data to Conformational Ensembles: Structurally and Dynamically based Methods*, preprint, ZIB SC 98-36.
- [2] F. Cordes, E. B. Starikov, W. Saenger, J. Am. Chem. Soc. 117, 10365 (1995).
- [3] A. Amadei, A. B. M. Linssen, H. J. C. Berendsen, Proteins 17, 412 (1995).

- [4] A. Frieze, R. Kannan, S. Vempala, *Fast Monte-Carlo Algorithms for finding low-rank approximations*, preprint, Yale University Computer Science Dept., <http://www.cs.yale.edu/users/kannan/Papers/cluster.ps>.
- [5] A. K. Jain, R. C. Dubes, *Algorithms for Clustering Data*, Prentice Hall, 1988.
- [6] M. R. Anderberg, *Cluster Analysis for Applications*, Academic Press, New York, 1973.
- [7] W. Donath, A. Hoffman, IBM Technical Disclosure Bulletin 15, 938 (1972).
- [8] W. Donath, A. Hoffman, IBM J. Res. Develop. 17, 420 (1973).
- [9] M. Fiedler, Czech. Math. J. 25(100), 607 (1975).
- [10] M. Fiedler, Czech. Math. J. 25(100), 619 (1975).
- [11] H. L. Gordon, R. J. Somorjai, Proteins 14, 249 (1992).
- [12] M. E. Karpen, D. J. Tobias, C. L. Brooks III, Biochemistry 32, 412 (1993).
- [13] P. Drineas, A. Frieze, R. Kannan, S. Vempala, V. Vinay, *Clustering in large graphs and matrices*, to appear in: Proc. of the Symposium on Discrete Algorithms, SIAM, 1999, <http://www.cs.yale.edu/users/kannan/Papers/cluster.ps>.
- [14] A. Fischer, F. Cordes, C. Schütte, J. Comput. Chem. 19, 1689 (1998).
- [15] W. F. van Gunsteren, S. R. Billeter, A. A. Eising, P. H. Hünenberger, P. Krüger, W. R. P. Scott, I. G. Tironi, *Biomolecular Simulation: The GROMOS96 Manual and User Guide*, vdf Hochschulverlag, Zürich 1996.
- [16] B. Hendrickson, R. Leland, SIAM J. Sci. Comput. 16(2), 452 (1995).
- [17] B. Hendrickson, SIAM J. Optimization 5(4), 835 (1995).